International Journal of Non-Linear Mechanics 47 (2012) 1–7

Contents lists available at SciVerse ScienceDirect

International Journal of Non-Linear Mechanics

journal homepage: www.elsevier.com/locate/nlm

The effect of the thermal conductivity and thickness of the wall on the nonlinear instability of a thin film flowing down an incline

L.A. Dávalos-Orozco

Instituto de Investigaciones en Materiales, Departamento de Polímeros, Universidad Nacional Autónoma de México, Ciudad Universitaria Circuito Exterior S/N, Delegación Coyoacán, 04510 México D.F., Mexico

ARTICLE INFO

Article history:
Received 13 December 2011
Received in revised form
24 February 2012
Accepted 25 February 2012
Available online 3 March 2012

Keywords:
Thin liquid film
Inclined plane
Wall heat conductivity
Wall thickness
Thermocapillarity

ABSTRACT

The nonlinear thermal instability of a thin liquid film falling down a heated wall is investigated. In particular, the heat conductivity and the thickness of the wall are taken into account. It is found that these two effects are represented by only one parameter which is the ratio of the nondimensional thickness of the wall and the nondimensional heat conductivity of the wall, that is d/Q_c. The longwave linear stability is described in a general form with respect to a wide range of values of this parameter in order to understand the behavior of the thin film. In the nonlinear case, the thin film instability is investigated in space and time for two examples of time dependent perturbations. The first one is at a perturbation frequency of 0.5 and the second one is at 2.5. The Reynolds numbers corresponding to the isothermal maximum growth rate are used and it is shown that they are located at important places of the k vs. R plane, where k is the wave number and R is the Reynolds number. It is found the important result that, for any fixed Marangoni number Ma, the increase of the parameter d/Q_c stabilizes the flow and at the same time decreases the nonlinear amplitude of the perturbations.

1. Introduction

Thin liquid films falling down walls have been investigated since many years ago due to their important applications in coating and heat dissipation problems. It is common in the literature to find results of their instability assuming from the onset that the wall is a very good thermal conductor. However, it is always supposed that the atmosphere on the other side of the film has different thermal conductivities. This is taken into account in the Biot number of the free surface, which is a nondimensional parameter representing the adimensional ratio of the coefficient of heat transfer times the thickness of the layer and divided by the thermal conductivity of the fluid. Here, in contrast to other papers in the literature, the goal is to understand the influence of the heat conductivity and thickness of the wall in the nonlinear instability of falling films.

The instability of thin films, investigated in isothermal conditions, has been reviewed by Weinstein and Ruschak [1], Quéré [2] and Oron et al. [3]. However, Oron et al. [3] also include a review of the thermal problem. A more recent review on isothermal and thermal instabilities has been presented by Craster and Matar [4]. The linear instability was investigated for small wave number and small Reynolds number approximations in a paper by Yih [5]. The shear soft and hard mode instabilities were investigated by De Bruin [6]. In order to understand the shear mode, Floryan et al. [7] investigated the instability for small angles of inclination. An evolution equation valid for order one Reynolds number was calculated by Benney [8]. This was solved with a normal mode approximation by Gjevik [9] who calculated for the first time the nonlinear curve of subcriticality. The three-dimensional version of the Benney equation was obtained by Roskes [10]. The relation of this equation with the Kuramoto–Sivashinsky equation was demonstrated by Sivashinsky and Michelson [11] for strong surface tension. The Benney equation was solved in space and time by Dávalos et al. [12] and extended to the case of flow on a rotating inclined wall by Dávalos and Busse [13]. Many thin films phenomena have large Reynolds number. Therefore, other approximate equations have to be calculated under different assumptions in the scaling. Examples of these efforts are given in Alekseenko et al. [14,15], Trifonov [16] and Chang [17].

The thermocapillary problem has been investigated by Kelly and Goussis [18], Kelly et al. [19] and Goussis and Kelly [20] who made calculations of the thermal and shear modes of instability. The nonlinear problem was solved numerically by means of a Benney-type equation by Joo et al. [21] and Joo and Davis [22]. Full numerical analysis for heated films has been investigated by Krishnamoorthy et al. [23], Ramaswamy [24] and Miyara [25]. Results of experiments on heated falling films have been done by Al-Sivai et al. [26] using an infrared thermography technique, by

E-mail address: ldavalos@unam.mx

0020-7462/$ - see front matter © 2012 Elsevier Ltd. All rights reserved.
doi:10.1016/j.ijnonlinmec.2012.02.008

Zaitsev and Kabov [27] using a 150 mm × 150 mm vertical heated plate in a vertical plane and by Stadler et al. [28] who were also interested on the thermal-capillary breakdown. Some theoretical advances were made by Kalliadasis et al. [29] using the Shkadov integral-boundary-layer approximation, by Trevelyan and Kalliadasis [30] making an approximation of large Péclet number, by Schied et al. [31] investigating the validity domain of the Benney model equation with Marangoni effects and by Ruyer-Quil et al. [32] and Schied et al. [33] by means of a gradient expansion along with a Galerkin projection with polynomial test functions. The results of the fixed temperature and fixed heat flux thermal boundary conditions have been compared by Trevelyan et al. [34]. Scheid et al. [35] obtained results on the thermal problem in three dimensions with emphasis on the formation of rivulets. Heat transfer in thin film problems have also been investigated taking into account the topography of the wall. Saprykin et al. [36] show in the lubrication approximation the formation of drops in the troughs of the wavy deformation of the wall. D'Alessio et al. [37] make a stability analysis of thin films falling down wavy walls and compare with solutions of the Navier–Stokes equations and experiments.

The thickness of the wall has been used in the nonlinear problem of thin films by some authors. Oron et al. [38] only used the thickness of the wall to eliminate singularities at rupture point in their problem of thermal and evaporative instabilities. Kabova et al. [39] used the thickness of the wall to allow for wall deformations in the side in contact with the liquid film. Gambaryan-Roisman [40] investigated the Marangoni instability of a liquid layer over a thick wall with variable thermal conductivity. However, the thickness of the wall is varied only assuming a relation with the thermal conductivity nonuniformity. Gambaryan-Roisman and Stephan [41] investigated the formation of rivulets in thin films flowing down a heated thick wall with topography and taking into account the Lennard–Jones potential.

In all the papers above, and to the author best knowledge, there is no systematic research taking into account the effect of the conductivity and thickness of the wall on the nonlinear instability of thin films flowing down. Therefore, the main goal of the paper is to investigate in detail the nonlinear instability of a heated liquid film flowing down a thick wall and to determine the limitations of the model evolution equation of the Benney type, which will be given presently.

The paper is organized as follows. In the next section, the perturbed Benney equation is presented including the Marangoni effects with the influence of the conductivity and thickness of the wall. In Section 3, numerical solutions of the equation are presented with illustrative examples corresponding to different values of the parameters. Sections 4 and 5 are the discussion and conclusions, respectively.

2. The perturbed Benney equation with Marangoni effects including the conductivity and thickness of the wall

The nonlinear evolution equation for the thin film is calculated under the lubrication approximation. In this approximation, it is supposed that the slope of the free surface waves is very small and therefore their wavelength is very large with respect to the wave amplitude. That is, $\varepsilon = 2\pi h_0/\lambda \ll 1$, where the thickness of the layer is h_0 and λ is the wavelength. The distances in the direction perpendicular to the wall and parallel to it are made nondimensional by means of h_0 and $\lambda/2\pi$, respectively. This will allow to make a scaling for the variation in different directions using ε. Time is made nondimensional with $h_0\lambda/(2\pi v)$, velocity with v/h_0, pressure with $\rho v^2/h_0^2$ and temperature with $\Delta T = (T_0 - T_{ambient}) > 0$. The properties of the fluid are the kinematic viscosity v and the density ρ. Here, T_0 is the temperature at the lower face of the wall and $T_{ambient}$ is the temperature of the ambient atmosphere above the fluid free surface.

The origin $z=0$ of the coordinate system is located at the upper side of the wall in contact with the fluid. If the unperturbed free surface is set at $z=1$, then the perturbed free surface is located at $z = 1 + H(x,y,t) = h(x,y,t)$. The wall lower face is found at $z = -d = -d_w/h_0$, where d_w is the thickness of the wall. The thin film moves down in the x-direction with the y-direction perpendicular to it, like in a right-handed system.

It is assumed that the pressure is p, the velocity components in the (x,y,z) directions are (u,v,w), the temperature is T, the angle of inclination of the wall is β, the Reynolds number is $R = gh_0^3/v^2$ and the Prandtl number is $Pr = v/\kappa$ with κ the heat diffusivity. Then, the scaled Navier–Stokes, continuity and heat diffusion equations are

$$\varepsilon u_t + \varepsilon u u_x + \varepsilon v u_y + w u_z = -\varepsilon p_x + \varepsilon^2 u_{xx} + \varepsilon^2 u_{yy} + u_{zz} + R\sin\beta, \tag{1}$$

$$\varepsilon v_t + \varepsilon u v_x + \varepsilon v v_y + w v_z = -\varepsilon p_y + \varepsilon^2 v_{xx} + \varepsilon^2 v_{yy} + v_{zz}, \tag{2}$$

$$\varepsilon w_t + \varepsilon u w_x + \varepsilon v w_y + w w_z = -p_z + \varepsilon^2 w_{xx} + \varepsilon^2 w_{yy} + w_{zz} - R\cos\beta, \tag{3}$$

$$w_z = -\varepsilon u_x - \varepsilon v_y, \tag{4}$$

$$Pr(\varepsilon T_t + \varepsilon u T_x + \varepsilon v T_y + w T_z) = \varepsilon^2 T_{xx} + \varepsilon^2 T_{yy} + T_{zz}. \tag{5}$$

Subindexes x, y, z and t mean partial derivatives. The boundary conditions are evaluated at the lower face of the wall, at the upper face of the wall and at the free surface. At the upper face of the wall, the nonslip condition is

$$u = v = w = 0 \quad \text{at } z = 0. \tag{6}$$

The normal stress boundary condition is

$$\begin{aligned} &-p + \frac{1}{N^2}[\varepsilon^3(u_x h_x^2 + v_y h_y^2) + \varepsilon^3(u_y + v_x)h_x h_y \\ &\quad -\varepsilon(v_z + \varepsilon w_y)h_y - \varepsilon(u_z + \varepsilon w_x)h_x + w_z] \\ &\quad = P_p(x,y,t) - \frac{3}{N^3}S[(1+\varepsilon^2 h_y^2)h_{xx} + (1+\varepsilon^2 h_x^2)h_{yy} - 2\varepsilon^2 h_x h_y h_{xy}] \\ &\quad \text{at } z = h(x,y,t), \end{aligned} \tag{7}$$

where $N = \sqrt{1+\varepsilon^2 h_x^2 + \varepsilon^2 h_y^2}$. The shear stresses are

$$\varepsilon(w_z - \varepsilon u_x)h_x - \frac{1}{2}\varepsilon^2(u_y + v_x)h_y + \frac{1}{2}(u_z + \varepsilon w_x)(1 - \varepsilon^2 h_x^2)$$

$$-\frac{1}{2}\varepsilon^2(\varepsilon w_y + v_z)h_x h_y = \frac{Ma}{Pr}(\varepsilon T_x + \varepsilon h_x T_z) \quad \text{at } z = h(x,y,t) \tag{8}$$

and

$$\varepsilon(w_z - \varepsilon u_y)h_y - \frac{1}{2}\varepsilon^2(u_y + v_x)h_x + \frac{1}{2}(v_z + \varepsilon w_y)(1 - \varepsilon^2 h_y^2)$$

$$-\frac{1}{2}\varepsilon^2(\varepsilon w_x + u_z)h_x h_y = \frac{Ma}{Pr}(\varepsilon T_y + \varepsilon h_y T_z) \quad \text{at } z = h(x,y,t). \tag{9}$$

The temperature conditions are

$$T_w = 1 \quad \text{at } z = -d,$$

$$T_w = T \quad \text{and} \quad Q_c dT_w/dz = dT/dz \quad \text{at } z = 0 \tag{10}$$

and

$$T_z + BiT = 0 \quad \text{at } z = h(x,y,t), \tag{11}$$

where T_w and T are the temperature distributions in the wall and the fluid, respectively, and Bi is the Biot number. The ratio of the wall and fluid heat conductivities is represented by $Q_c = k_w/k_f$.

The kinematic boundary condition is

$$w = \varepsilon h_t + \varepsilon u h_x + \varepsilon v h_y \quad \text{at } z = h(x,y,t). \tag{12}$$

A pressure of the form

$$P_p(x,y,t) = A\left|\sin\frac{\omega}{2}t\right| \exp[-a(x^2+y^2)] \tag{13}$$

appears in the normal stress boundary condition equation (7). This is supposed to be an external pressure due to a turbulent air jet which strikes periodically at the origin on the free surface. For applications of a nonoscillating turbulent air jet see Lacanette et al. [42]. The constants of the pressure p_p in Eq. (13) will be taken as $A=0.0001$ and $a=0.05$. The magnitudes were selected because it was found that the film instability is very sensitive to these parameters. The frequency of oscillation ω is divided by two because a jet has no suction and it will have effect only when it strikes again on the surface.

Because the surface tension is assumed strong, the nondimensional surface tension number $\Sigma=\sigma h_0/(3\rho\nu^2)$ is changed into $S=\varepsilon^2\Sigma$ when the scaling is used. For the thermal effects in the liquid, there are two other parameters. They are the Marangoni number $Ma=(-d\sigma/dT)\Delta T h_0/(\rho\nu\kappa)$ and the Biot number $Bi=H_h h_0/k_f$, where H_h is the coefficient of heat transfer.

The expansion of the variables is made according to the lubrication approximation. In that sense, the z-component of the velocity is very slow as seen below:

$$u=u_0+\varepsilon u_1+\cdots,\quad v=v_0+\varepsilon v_1+\cdots,\quad w=\varepsilon(w_1+\varepsilon w_2+\cdots),$$

$$p=p_0+\varepsilon p_1+\cdots,\quad T=T_0+\varepsilon T_1+\cdots,\quad T_w=T_{w0}+\varepsilon T_{w1}+\cdots. \tag{14}$$

It is assumed that the three components of the velocity, the pressure and the temperatures of the wall T_w and the fluid T, depend on (x,y,z,t). The free surface height h only depends on (x,y,t). Then, these expansions are used in all the equations and the boundary conditions. To zeroth order the results are

$$p_0=-(z-h)R\cos\beta-3S\nabla^2 h+P_p(x,y,t), \tag{15}$$

$$u_0=-\tfrac{1}{2}R\sin\beta z(z-2h), \tag{16}$$

$$w_1=-\tfrac{1}{2}R\sin\beta z^2 h_x, \tag{17}$$

$$T_0=\frac{Q_c(1+Bih)-BiQ_c z}{Q_c(1+Bih)+Bid},\quad T_{w0}=\frac{Q_c(1+Bih)-Biz}{Q_c(1+Bih)+Bid}, \tag{18}$$

$$h_t=-R\sin\beta h^2\frac{\partial h}{\partial x}\quad \text{at } z=h(x,y,t). \tag{19}$$

No more terms of the expansion of T are needed due to the scaling in the shear stress boundary conditions and therefore only T_0 in Eq. (18) will be used. Its effects will appear in the solutions at first order.

The results to first order are

$$u_1=\frac{1}{24}z\Big[(R\sin\beta)^2(z^3-4h^3)hh_x+R\sin\beta(4z^2-12h^2)h_t +12(z-2h)p_{0x}+24\frac{Ma}{Pr}\left(\frac{Bi(d+Q_c h)}{Q_c(1+Bih)+Bid}\right)_x\Big], \tag{20}$$

$$v_1=\frac{1}{2}z\left[(z-2h)p_{0y}+2\frac{Ma}{Pr}\left(\frac{Bi(d+Q_c h)}{Q_c(1+Bih)+Bid}\right)_y\right], \tag{21}$$

$$w_2=\frac{1}{120}z^2\Big[(R\sin\beta)^2((10h^4-z^3h)h_x)_x+R\sin\beta((30h^2-5z^2)h_t)_x -60\frac{Ma}{Pr}\nabla^2\left(\frac{Bi(d+Q_c h)}{Q_c(1+Bih)+Bid}\right)+60\nabla\cdot\left(\left(h-\frac{1}{3}z\right)\nabla p_0\right)\Big], \tag{22}$$

Notice that $\nabla=(\partial/\partial x,\partial/\partial y)$ is the horizontal nabla operator and that h_t which appears above will be replaced by the zeroth order approximation of the kinematic boundary condition equation (19). The above results are substituted in the kinematic boundary condition at first order to give the following Benney-type equation for the evolution of the free surface waves of a fluid film flowing down a wall with finite thickness and thermal conductivity. That is

$$h_t+R\sin\beta h^2 h_x+\varepsilon\Bigg\{(R\sin\beta)^2\left(\frac{2}{15}h^6 h_x\right)_x +\frac{1}{3}\nabla\cdot\Bigg[h^3(-R\cos\beta\nabla h+3S\nabla^2\nabla h-\nabla P_p) +\frac{1}{2}\frac{Ma}{Pr}\frac{Bih^2}{\left(1+Bih+Bi\left(\frac{d}{Q_c}\right)\right)^2}\nabla h\Bigg]\Bigg\}=0. \tag{23}$$

The above equation reduces to that of Joo et al. [21], but in the absence of evaporation, when $d=0$ and $P_p=0$. In their paper [21], they use the inverse of the Biot number defined here.

The linear version of Eq. (23) can be calculated dropping the scaling and using $h=1+H(x,t)$, where $H(x,t)=A_1\exp i[\vec{k}\cdot\vec{x}-(i\Gamma+\omega)t]$ and A_1 is a small constant amplitude. The definitions of the terms in the exponent are $\vec{x}=(x,y)$, the wave number vector $\vec{k}$ (with magnitude k), the growth rate Γ and the frequency of oscillation ω. From the results of the imaginary part, it is found that the phase velocity is $c=\omega/k=R\sin\beta$. The real part gives the growth rate:

$$\Gamma=k^2\left(\frac{2R^2\sin^2\beta}{15}-\frac{1}{3}R\cos\beta-k^2\Sigma+\frac{1}{6}\frac{Ma}{Pr}\frac{Bi}{\left(1+Bi+Bi\left(\frac{d}{Q_c}\right)\right)^2}\right). \tag{24}$$

When the growth rate is zero the curve of criticality is

$$k_c=\sqrt{\frac{1}{\Sigma}\left(\frac{2}{15}R^2\sin^2\beta-\frac{1}{3}R\cos\beta+\frac{1}{6}\frac{Ma}{Pr}\frac{Bi}{\left(1+Bi+Bi\left(\frac{d}{Q_c}\right)\right)^2}\right)}. \tag{25}$$

We have shown analytically that the wave number of the maximum growth rate and that of subcriticality [9] satisfy, respectively, the relations $k_m=k_c/\sqrt{2}$ and $k_s=k_c/2$. Notice that these relations are the same as in the isothermal case. Below the curve of subcriticality k_s, saturation of the perturbation waves is not expected. The above results can be reviewed as:

$$k_c=\sqrt{2}k_m=2k_s \tag{26}$$

In Fig. 1a, a three-dimensional plot of the function $f(d/Q_c,Bi)=Bi/(1+Bi+Bi(d/Q_c))^2$ which determines the influence of thermocapillary effects on the thin film instability is shown. This function has a maximum $1/4(1+d/Q_c)$ with respect to the Bi at $Bi_{max}=1/(1+d/Q_c)$. These two reduce to $1/4$ and $Bi_{max}=1$, respectively, for the fixed temperature boundary condition at the wall, which corresponds to $d=0$ (or else $Q_c\to\infty$). In this paper, the Biot number will be fixed at $Bi=0.1$ and the function $f(d/Q_c,Bi)$ will depend only on d/Q_c, as shown in Fig. 1b, which represents a section of the surface in Fig. 1a.

The k vs. R curves of criticality, maximum growth rate and subcriticality are plotted in Fig. 2 for fixed $\beta=90^\circ$, $Pr=7$ and $S=1$ and for three different magnitudes of Ma: (a) $Ma=25$, (b) $Ma=50$, (c) $Ma=100$. The curves are presented for five different magnitudes of d/Q_c: (1) $d/Q_c=0.01$, (2) $d/Q_c=0.1$, (3) $d/Q_c=1$, (4) $d/Q_c=10$, (5) $d/Q_c=100$. As seen in the figure, the curves of $d/Q_c=0.01$ and 0.1 are almost the same.

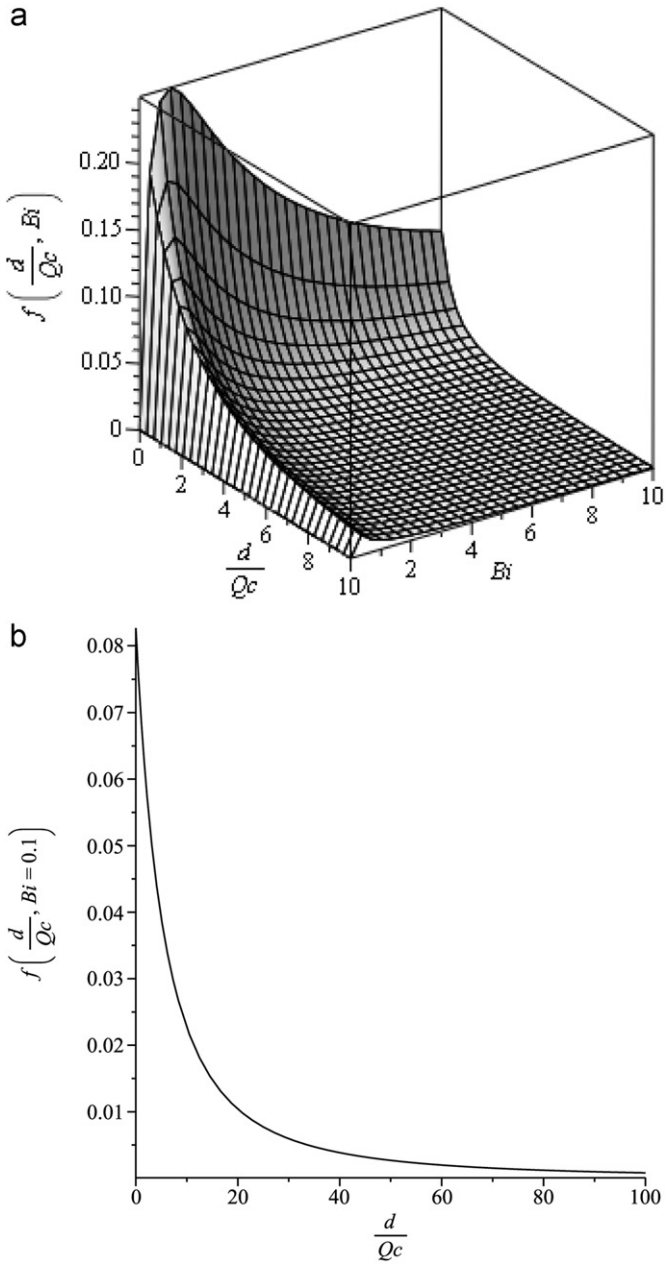

Fig. 1. (a) Three-dimensional plot of the function $f(d/Q_c,Bi)=Bi/(1+Bi+Bi(d/Q_c))^2$. (b) Here, use will be made of $Bi=0.1$ and $f(d/Q_c,Bi=0.1)$.

The straight dot-dashed line shown in all the figures in Fig. 2, is the result of the maximum growth rate of the perturbations in the isothermal problem. Those lines are important because they will be used as reference in the numerical analysis of Eq. (23).

3. Numerical analysis of the Benney-type Eq. (23)

In this section, Eq. (23) will be analyzed numerically fixing some of the parameters of the problem. It will be assumed that the fluid is water and therefore $Pr=7$. The surface tension number is set as $S=1$ and the wall is vertical with $\beta=90^\circ$. The numerical calculations are done in space and time and the spatial range is determined starting at $x=-100$ and finishing at $R\Delta t+100$ (as found above, the phase velocity is $R\sin\beta$). Therefore, the product of the phase velocity by the time interval gives the total space range of the calculation. The time dependent perturbations due to

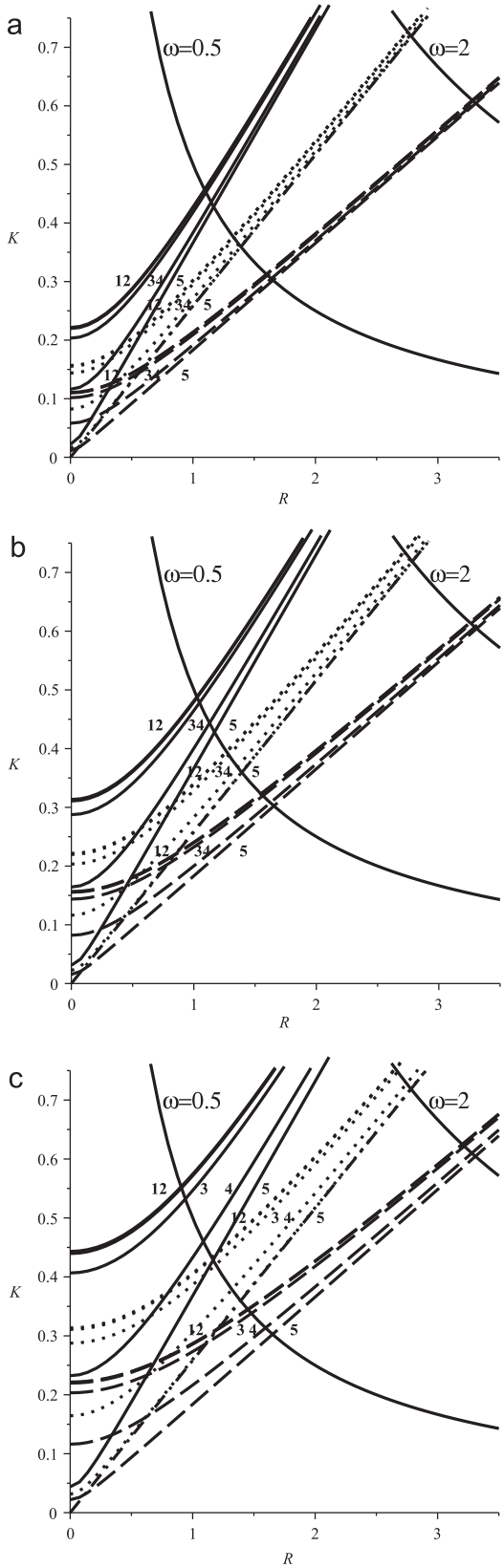

Fig. 2. $\beta=90^\circ$, $Pr=7$, $\Sigma=1$, $Bi=0.1$. (a) $Ma=25$, (b) $Ma=50$, (c) $Ma=100$. The solid, dotted and dashed curves correspond to the curves of criticality, maximum growth rate and subcriticality, respectively. The straight dot-dashed ones are the maximum growth rate of the isothermal problem used as reference for numerical results. The numbers in the curves indicate (1) $d/Q_c=0.01$, (2) $d/Q_c=0.1$, (3) $d/Q_c=1$, (4) $d/Q_c=10$, (5) $d/Q_c=100$. The curves of $d/Q_c=0.01$ and 0.1 are almost superposed. The hyperbolas $k=\omega/R$ are drawn for $\omega=0.5$ and 2.

a gas jet are applied at $x=0$. Thus, the initial point of spatial calculation $x=-100$ is set to avoid numerical reflection of the perturbation. The same can be said about the 100 added to the last point of the spatial calculation.

The Reynolds number and the frequency of oscillation of the perturbation used in the numerical analysis will always correspond to the maximum growth rate of the perturbation in the isothermal case. This will be useful as reference when the Marangoni number is changed. In this way, the expression "the system moves" will be used to indicate the relative motion a point has in the dot-dashed line when Ma increases or d/Q_c decreases. For example, if Ma increases, a great part of the dot-dashed line moves inside the region of subcriticality and saturation is difficult to attain (see Fig. 2a–c). Moreover, if at the same time d/Q_c decreases, another section of the dot-dashed line moves inside the region of subcriticality (see how the dashed lines in Fig. 2a–c increase their height when d/Q_c decreases, from curves 5 to 1).

Two frequencies of oscillation have been selected to understand the behavior of the system when the thickness and thermal conductivity of the wall are taken into account. They are $\omega=0.5$ and $\omega=2$. The reason is that for $\omega=0.5$, it is easier to the system to move near the curve of subcriticality when Ma increases, in comparison with the case $\omega=2$. In this sense, the Reynolds number has a stabilizing effect (see in Fig. 2 the points at which the hyperbolas $k=\omega/R$ for $\omega=0.5$ and $\omega=2$ cross the dot-dashed lines of the isothermal maximum growth rate).

The first results, shown in Fig. 3, are for $Ma=25$, an external perturbation frequency $\omega=0.5$ and $R=1.391$. In this case, the time of the calculation is $T=1000$. From the figure, it is seen that good convergence is attained for the five values of the parameter d/Q_c. The amplitude of the nonlinear wave increases when d/Q_c decreases. Small wave modulation is seen for the perturbations of largest amplitude.

For the same Marangoni number but $\omega=2$ and $R=2.783$, Fig. 4 shows the solution for a time $T=600$. It is clear that the amplitude of the perturbations decreases with the increase of d/Q_c, but here it is not very effective. No modulation is found in all the space interval.

The increase of the Marangoni number to $Ma=50$ produces strong wave modulation as seen in Fig. 5 for $\omega=0.5$ and $R=1.391$ and time $T=1000$. However, this modulation disappears along with a decrease in amplitude due to the growth of d/Q_c. Saturation is very good.

When the frequency is $\omega=2$ and the Reynolds number is $R=2.783$, Fig. 6 shows results for $T=600$ and $Ma=50$. It is clear from the figure that without the stabilizing effect of d/Q_c the saturation of the perturbation in space is difficult to attain. Saturation is seen only for $d/Q_c=1,10$ and 100.

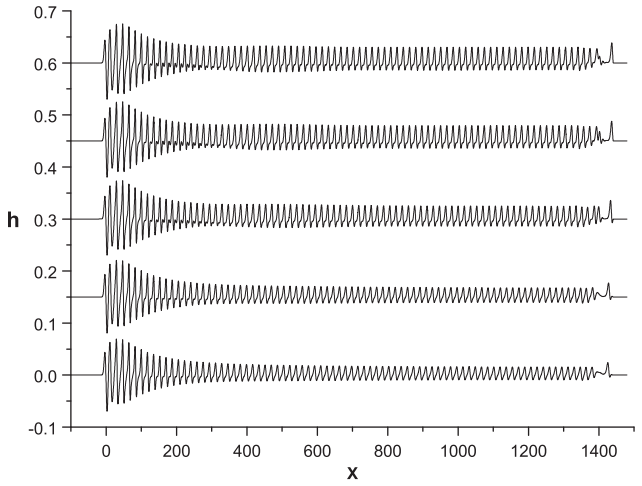

Fig. 3. $\beta=90^\circ$, $\varepsilon=0.1$, $Pr=7$, $S=1$, $Bi=0.1$ and $Ma=25$. Here, $\omega=0.5$, $R=1.391$ and the calculation time is $T=1000$. From above to below, the curves represent free surface perturbations corresponding to $d/Q_c=$ 0.01, 0.1, 1, 10 and 100.

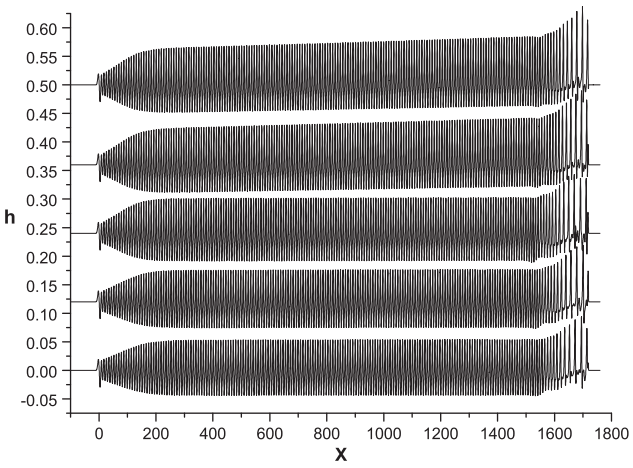

Fig. 4. $\beta=90^\circ$, $\varepsilon=0.1$, $Pr=7$, $S=1$, $Bi=0.1$ and $Ma=25$. Here, $\omega=2$ and $R=2.783$ and the calculation time is $T=600$. From above to below, the curves represent free surface perturbations corresponding to $d/Q_c=$ 0.01, 0.1, 1, 10 and 100.

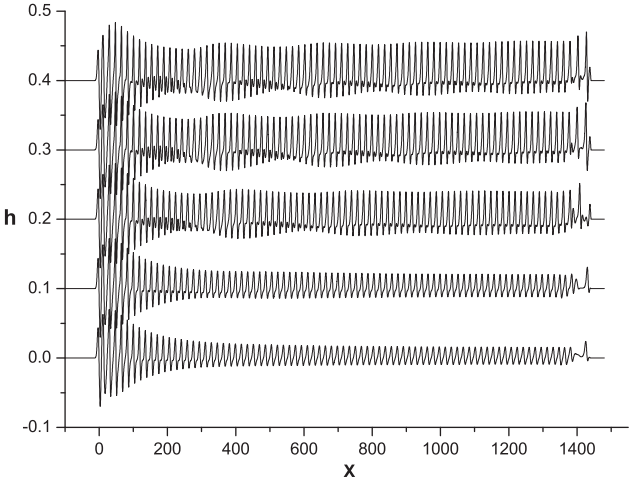

Fig. 5. $\beta=90^\circ$, $\varepsilon=0.1$, $Pr=7$, $S=1$, $Bi=0.1$ and $Ma=50$. Here, $\omega=0.5$ and $R=1.391$ and the calculation time is $T=1000$. From above to below, the curves represent free surface perturbations corresponding to $d/Q_c=$ 0.01, 0.1, 1, 10 and 100.

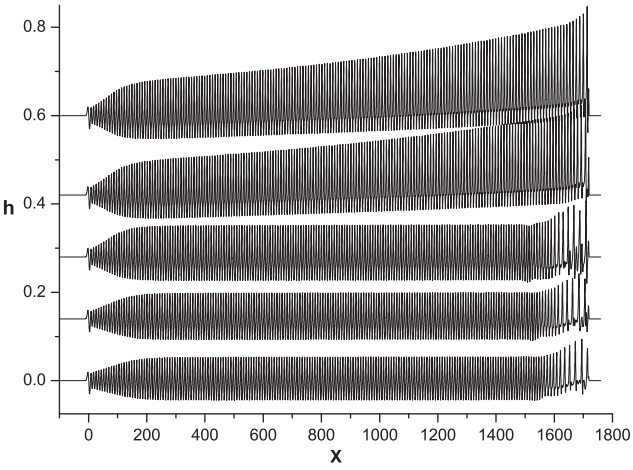

Fig. 6. $\beta=90^\circ$, $\varepsilon=0.1$, $Pr=7$, $S=1$, $Bi=0.1$ and $Ma=50$. Here, $\omega=2$ and $R=2.783$ and the calculation time is $T=600$. From above to below, the curves represent free surface perturbations corresponding to $d/Q_c=$ 0.01, 0.1, 1, 10 and 100.

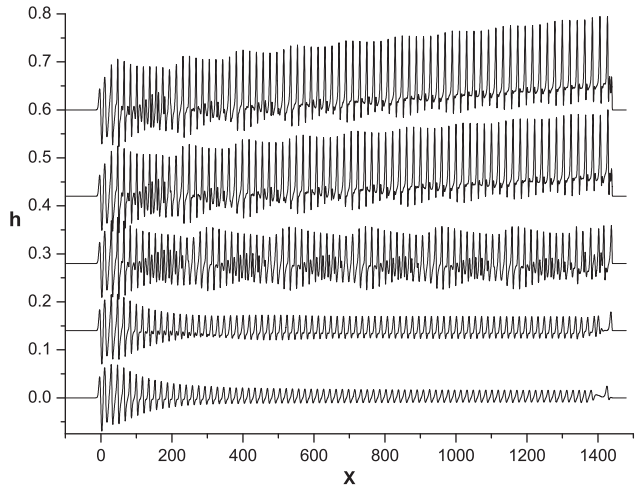

Fig. 7. $\beta=90^{\circ}$, $\varepsilon=0.1$, $Pr=7$, $S=1$, $Bi=0.1$ and $Ma=100$. Here, $\omega=0.5$ and $R=1.391$ and the calculation time is $T=1000$. From above to below, the curves represent free surface perturbations corresponding to $d/Q_c=$ 0.01, 0.1, 1, 10 and 100.

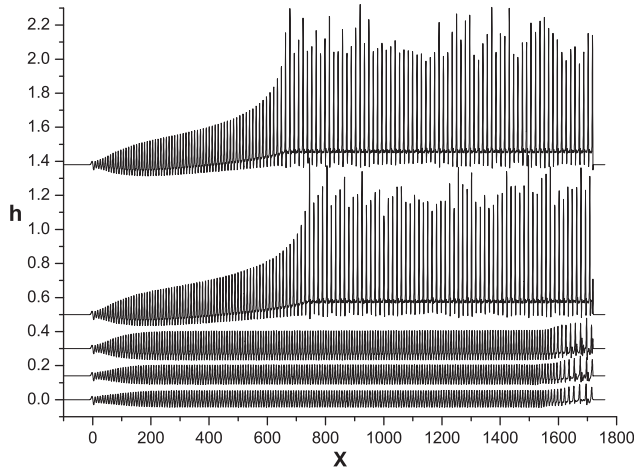

Fig. 8. $\beta=90^{\circ}$, $\varepsilon=0.1$, $Pr=7$, $S=1$, $Bi=0.1$ and $Ma=100$. Here, $\omega=2$ and $R=2.783$ and the calculation time is $T=600$. From above to below, the curves represent free surface perturbations corresponding to $d/Q_c=$ 0.01, 0.1, 1, 10 and 100.

A further increase of Marangoni number until $Ma=100$ leads to the results of Fig. 7. Here, $\omega=0.5$ and $R=1.391$ and the calculation time is $T=1000$. The spatial modulation now extends up to the magnitude $d/Q_c=1$. However, very good saturation is obtained only for $d/Q_c\geq 1$, magnitudes at which the perturbations amplitudes decrease considerably.

As can be seen in Fig. 8, the increase of the Marangoni number to a magnitude of $Ma=100$ has important consequences when $\omega=2$, $R=2.783$ and $T=600$. It is found that numerical convergence is very difficult to attain for $d/Q_c\leq 0.1$. However, when $d/Q_c\geq 1$ numerical convergence and saturation are very well satisfied. It is clear that spatial modulation is not present in any of the numerical solutions.

4. Discussion

The results presented in the figures show that the variation of d/Q_c changes the nonlinear instability of the flow. The increase of d/Q_c means that the thickness of the wall increases with respect to that of the film, or else, that the thermal conductivity of the wall is decreasing in magnitude with respect to that of the film. This increase in d/Q_c was shown to be stabilizing because it decreases the magnitude of the coefficient of the thermocapillary term, as can be seen in Fig. 1a and b. Therefore, with $d/Q_c\to\infty$ the nonlinear instability of the flow with Marangoni effects tends to become the isothermal one. That is the reason why the amplitude of the time dependent perturbations decreases with respect to that of $d/Q_c\to 0$.

Note that the selected values of $\omega=0.5$ and $R=1.391$ always remain above the curves of subcriticality for the Marangoni numbers used here, as seen in Fig. 2a–c. However, when $Ma=100$ the numerical solutions have no saturation for $d/Q_c=0.01,0.1$. They were expected to have saturation in this case because Dávalos-Orozco et al. [12] found saturation below but near the curve of subcriticality in the isothermal flow.

From Fig. 6, it is clear that saturation is not attained for $\omega=2$ and $R=2.783$ despite $Ma=50$ and $d/Q_c=0.01,0.1$. This is surprising because in Fig. 2a–c, the corresponding point is far above the curve of subcriticality. Then, for this Reynolds number the thermocapillary effects have a very strong destabilizing effects. Moreover, the results of Fig. 8 for $Ma=100$ show that convergence is very bad when $d/Q_c=0.01,0.1$. This means that, in the thermal case, the Benney-type equation model is not good for these magnitudes of the Marangoni and Reynolds numbers. Moreover, it is found that the validity region of that model is more reduced, in the k vs. R plane, in comparison with the isothermal case (see [12]).

5. Conclusions

In contrast with papers published before [38–41], here we present the results related explicitly with the geometry and thermal properties of the wall. It is shown that the influences of the thickness of the wall and its thermal conductivity are important in determining the nonlinear instability of the thin film flowing down a heated wall. The role played by the ratio d/Q_c has been made clear numerically. A very important result of the paper is that for large magnitudes of the Marangoni number nonlinear saturation can always be attained for large enough magnitudes of d/Q_c. In the figures, it is noted that the amplitude of the perturbations decreases with an increase of d/Q_c and spatial modulation disappears. From the analysis, it is found that the magnitude of the thermocapillary term decreases when d/Q_c increases and that, for this reason, the nonlinear instability tends to that of the isothermal problem. Therefore, it is possible to conclude that to avoid the effect of thermocapillary perturbations the wall has to have the thermal properties and geometry corresponding to large d/Q_c. In this way, the perturbations propagating on the free surface will be nearly isothermal.

From the results of the paper, it is concluded that it is necessary to review the region of validity of the Benney equation, as done by Scheid et al. [31], in terms of the new parameters of the heated system. The thermal boundary condition used at the wall by Scheid et al. [31] was that of fixed temperature. The stabilizing effects of the thickness and conductivity of the wall are apparent from the results presented above, and there is the possibility that these effects are also reflected in the validity of the Benney equation when the thermal problem becomes nearly isothermal, even for high temperature differences.

Acknowledgments

The authors would like to thank Joaquín Morales, Cain González, Raúl Reyes, Ma. Teresa Vázquez and Oralia Jiménez for technical support.

References

[1] S.J. Weinstein, K.J. Ruschak, Annual Review of Fluid Mechanics 36 (2004) 29.
[2] D. Quéré, Annual Review of Fluid Mechanics 31 (1999) 347.
[3] A. Oron, S.H. Davis, S.G. Bankoff, Reviews of Modern Physics 69 (1997) 3.
[4] R.V. Craster, O.K. Matar, Reviews of Modern Physics 81 (2009) 1131.
[5] C.-S. Yih, Physics of Fluids 6 (1963) 321.
[6] G.D. De Bruin, Journal of Engineering Mathematics 8 (1974) 259.
[7] J.M. Floryan, S.H. Davis, R.E. Kelly, Physics of Fluids 30 (1987) 983.
[8] D.J. Benney, Journal of Mathematical Physics 45 (1966) 150.
[9] B. Gjevik, Physics of Fluids 13 (1970) 1918.
[10] G.J. Roskes, Physics of Fluids 13 (1970) 1440.
[11] G.I. Sivashinsky, D.M. Michelson, Progress of Theoretical Physics 63 (1980) 2112.
[12] L.A. Dávalos-Orozco, S.H. Davis, S.G. Bankoff, Physical Review E 55 (1997) 374.
[13] L.A. Dávalos-Orozco, F.H. Busse, Physical Review E 65 (2002) 026312.
[14] S.V. Alekseenko, V.Y. Nakoryakov, B.G. Pokusaev, AIChE Journal 31 (1985) 1446.
[15] S.V. Alekseenko, V.Ye. Nakoryakov, B.G. Pokusaev, Wave Flow of Liquid Films, Begell House, Inc., New York, 1994.
[16] Y.Y. Trifonov, Russian Journal of Engineering Thermophysics 1 (1991) 153.
[17] H.-C. Chang, Annual Review of Fluid Mechanics 26 (1994) 103.
[18] R.E. Kelly, D.A. Goussis, Instability of a liquid film flowing down a heated inclined plane, in: U. Grigull, E. Hahne, K. Stephan, J. Straub (Eds.), Heat Transfer 1982, Proceedings of the Seventh International Heat Transfer Conference, vol. 5, Hemisphere, New York, 1982, p. 319.
[19] R.E. Kelly, S.H. Davis, D.A. Goussis, On the instability of heated film flow with variable surface tension, in: C.L. Tien, V.P. Carey, J.K. Ferrell (Eds.), Heat Transfer 1986, Proceedings of the Eighth International Heat Transfer Conference, vol. 4, Hemisphere, New York, 1986, p. 1937.
[20] D.A. Goussis, R.E. Kelly, Journal of Fluid Mechanics 223 (1991) 25.
[21] S.W. Joo, S.H. Davis, S.G. Bankoff, Journal of Fluid Mechanics 230 (1991) 117.
[22] S.W. Joo, S.H. Davis, Journal of Fluid Mechanics 242 (1992) 529.
[23] S. Krishnamoorthy, B. Ramaswamy, S.W. Joo, Physics of Fluids 7 (1995) 2291.
[24] B. Ramaswamy, S. Krishnamoorthy, S.W. Joo, Journal of Computational Physics 131 (1997) 70.
[25] A. Miyara, Heat Mass Transfer 35 (1999) 298.
[26] F. Al-Sibai, A. Leefken, U. Renz, International Journal of Thermal Sciences 41 (2002) 658.
[27] D.V. Zaitsev, O.A. Kabov, Experiments in Fluids 39 (2005) 712.
[28] V. Lel, H. Stadler, A. Pavlenko, R. Kneer, Heat Mass Transfer 43 (2007) 1121.
[29] S. Kalliadasis, E.A. Demekhin, C. Ruyer-Quil, M.G. Velarde, Journal of Fluid Mechanics 492 (2003) 303.
[30] P.M.J. Trevelyan, S. Kalliadasis, Journal of Engineering Mathematics 50 (2004) 177.
[31] B. Scheid, C. Ruyer-Quil, U. Thiele, O.A. Kabov, J.C. Legros, P. Colinet, Journal of Fluid Mechanics 527 (2005) 303.
[32] C. Ruyer-Quil, B. Scheid, S. Kalliadasis, M.G. Velarde, R.K. Zeytounian, Journal of Fluid Mechanics 538 (2005) 199.
[33] B. Scheid, C. Ruyer-Quil, S. Kalliadasis, M.G. Velarde, R.K. Zeytounian, Journal of Fluid Mechanics 538 (2005) 223.
[34] P.M.J. Trevelyan, B. Scheid, C. Ruyer-Quil, S. Kalliadasis, Journal of Fluid Mechanics 592 (2007) 295.
[35] B. Scheid, S. Kalliadasis, C. Ruyer-Quil, P. Colinet, Physical Review E 78 (2008) 066311.
[36] S. Saprykin, P.M.J. Trevelyan, R.J. Koopmans, S. Kalliadasis, Physical Review E 75 (2007) 026306.
[37] J.D. D'Alessio, J.P. Pascal, H.A. Jazmine, K.A. Ogden, Journal of Fluid Mechanics 665 (2010) 418.
[38] A. Oron, S.G. Bankoff, S.H. Davis, Physics of Fluids 8 (1996) 3434.
[39] Y.O. Kabova, A. Alexeev, T. Gambarian-Roisman, P. Stephan, Physics of Fluids 18 (2006) 012104.
[40] T. Gambaryan-Roisman, International Journal of Heat Mass Transfer 53 (2010) 390.
[41] T. Gambaryan-Roisman, P. Stephan, Journal of Heat Transfer 131 (2010) 033101.
[42] D. Lacanette, A. Gosset, S. Vincent, J-M. Buchlin, E. Arquis, Physics of Fluids 18 (2006) 042103.